# Heavy-quark potentials in the gluon plasma.
# Analysis of the singlet and octet channels

Mark I. Gorenstein [1], Walter Greiner
*Institut für Theoretische Physik der J.W. Goethe Universität, Postfach 111932, W-6000 Frankfurt am Main 11, FRG*

and

Stanisław Mrówczyński
*Soltan Institute for Nuclear Studies, ul. Hoża 69, PL-00-681 Warsaw, Poland*

We analyse the Monte Carlo lattice data for the heavy-quark potentials in the SU(3) gluon plasma and find out that non-perturbative effects are very different for singlet and octet $Q\bar{Q}$ colour channels. The data are analysed within a plasma model, where low-momentum gluons are converted into colourless modes and consequently are absent in the spectrum of deconfined gluons.

It is expected from the asymptotic freedom of quantum chromodynamics that at extremely high temperatures and/or baryonic densities the quark–gluon plasma (QGP) can be described as a system of weakly interacting quarks and gluons. However, at conditions achievable in real experiments on heavy-ion collisions, QGP can be formed only near the boundary of the phase transition to the "hadron gas". Thus, the standard perturbative approach to QGP is surely inadequate in this case and even elementary modes of QGP excitation are not known [1].

Monte Carlo (MC) simulations of lattice gauge theories are the important quantitative method to study non-perturbative effects in QGP. And indeed, the MC data on the thermodynamical functions (energy density, pressure) of the SU(2) [2] and SU(3) [3] gluon plasma (GP) manifest non-perturbative effects, particularly evident in the temperature interval between $T_c$ and $2T_c$, where $T_c$ is the deconfinement transition temperature. To explain the main features of these data a simple ("cut-off") model was proposed [2,4–7], where gluons with momentum smaller than a critical value $K$ are converted into colourless modes, and consequently do not appear in the spectrum of deconfined gluons. This model was further used [8] to describe the MC data of the potential acting between heavy quark and antiquark ($Q\bar{Q}$) in the SU(2) [9] and SU(3) [10] GP. The description of the SU(2) data was very successful, while the analysis of the SU(3) data appeared rather inconclusive. In the present paper we continue this study and consider SU(3) data [10] in more detail. A new aspect of our analysis is the investigation of separate colour channels. We find out rather different non-perturbative effects in the heavy-quark potentials for singlet and octet $Q\bar{Q}$ colour states. This fact happens to be crucial for the colour-averaged potential which is more sensitive to the non-perturbative effects than the singlet and octet potentials. For this reason the perturbative relations for colour-averaged potential [11] are strongly violated (see ref. [10]).

The $Q\bar{Q}$ system can be in $N_c \times N_c = 9$ different colour states which are decomposed into 1 singlet (colourless) state and 8 adjoint (colour) states. We denote corresponding singlet and octet $Q\bar{Q}$ potentials

[1] Permanent address: Institute for Theoretical Physics, 252130 Kiev-130, Ukraine.

as $V_1 \equiv V_{singl}$ and $V_8 \equiv V_{adj}$. The averaging over colour orientations gives a colour-averaged potential $V$ [11]:

$$\exp\left(-\frac{V(r,T)}{T}\right) = \tfrac{1}{9}\exp\left(-\frac{V_1(r,T)}{T}\right)$$
$$+ \tfrac{8}{9}\exp\left(-\frac{V_8(r,T)}{T}\right), \tag{1}$$

where $r$ is the distance between Q and $\bar{Q}$, $T$ is the temperature of the GP. MC calculations [10] were made, in fact, for $V$ and $V_1$ ($V_8$ is calculated then from eq. (1)). $T$ and $r$ are measured on the lattice of size $N_\sigma^3 \times N_\tau$ in units of the lattice spacing $a$:

$$T = \frac{1}{N_\tau a}, \quad r = a, 2a, ..., \tfrac{1}{2}N_\sigma a,$$

(the upper limit for $r$ arises because of the periodic boundary conditions). In the dimensionless variable $rT$ the interquark distance on a $12^3 \times 4$ lattice can be 0.25, 0.5, ..., 1.5. To avoid the problem with large finite size effects when $r$ is near its maximum value $\tfrac{1}{2}N_\sigma a$ (see ref. [9]) we do not analyse MC data [10] for $rT = 1.25, 1.5$.

The MC data of ref. [10] correspond to the three values of lattice coupling constant $g_L^2$: $6/g_L^2 = 5.75$, 6.10, 8.00. The deconfinement phase transition on a $12^3 \times 4$ lattice occurs at $6/\bar{g}_L^2 = 5.69$. To connect $g_L^2$ with $T$ we use the $g_L^2(a)$ function proposed in ref. [12] which takes into account the observed scaling violation. It gives (see ref. [7] for details) the following values of $T$ in units of $T_c$: $T/T_c = 1.16$, 2.2, 22.0.

The lowest order perturbative results for $V_1$ and $V_8$ are [11]

$$-V_1(r,T) = \frac{g^2}{4\pi} \cdot \frac{4}{3}\frac{\exp(-m_D r)}{r}, \tag{2}$$

$$V_8(r,T) = \frac{g^2}{4\pi} \cdot \frac{1}{6}\frac{\exp(-m_D r)}{r}, \tag{3}$$

where $g$ is the coupling constant

$$\frac{g^2}{4\pi} = \frac{4\pi}{11\ln(M^2/\Lambda^2)} \tag{4}$$

($\Lambda$ is the QCD scale parameter) and $m_D$ is the Debye screening mass. We define the mass parameter $M$ in (4) as [13]

$$M^2 = \frac{4}{3}\frac{\int_0^\infty k^2\,dk\,k^2 f_g(k)}{\int_0^\infty k^2\,dk\,f_g(k)}, \tag{5}$$

where $f_g(k)$ is the gluon distribution function ($k \equiv |\boldsymbol{k}|$). The Debye screening mass in the GP can be found in the framework of the kinetic approach [14,15] as

$$m_D^2 = -\frac{3g^2}{\pi^2}\int_0^\infty k^2\,dk\,\frac{\partial f_g(k)}{\partial k}. \tag{6}$$

Expressing $T_c$ in units of lattice scale parameter $\Lambda_L$ and using the relation $\Lambda = 83.5\Lambda_L$ [16] we find for the continuum scale parameter $\Lambda = 1.48T_c$. Therefore all physical quantities in our consideration are expressed in units of $T_c$ (the physical value of $T_c$ in real units, say MeV, remains unfixed).

According to the cut-off model [2,4–8] we choose the gluon distribution function in the form

$$f_g(k) = \frac{\theta(k-K)}{\exp(k/T)-1}, \tag{7}$$

which assumes that there are no gluons with momenta smaller than $K$, while the gluons with momenta larger than $K$ behave as in perturbative GP (see also ref. [17]). Thus formulae (2)–(6) are expected to be valid in spite of a (non-perturbative) modification of the gluon distribution. Consequently, the general perturbative relations [11]

$$-\frac{V_1(r,T)}{V_8(r,T)} = 8, \tag{8}$$

$$-\frac{V_1^2(r,T)}{TV(r,T)} = 16 \tag{9}$$

should be valid in the cut-off model too (the perturbative corrections are $O(g^4)$ to (8) and $O(g^2)$ to (9)).

Substituting (7) into (6) we find ($A \equiv K/T$)

$$m_D^2(T) = \frac{3}{\pi^2}g^2T^2\left(\int_A^\infty \frac{dx\,x^2\,e^x}{(e^x-1)^2} - \frac{A^2}{e^A-1}\right). \tag{10}$$

For $K/T \to 0$ we have $m_D(T) = gT$, which coincides with the standard perturbative result [11].

In fig. 1 we show the temperature dependence of $m_D/T$ for $K=0$ (the standard perturbative result), and $K = T_c$, $2T_c$, $6T_c$ (as explained above we fix $\Lambda = 1.48T_c$). One observes in fig. 1 that $m_D$ becomes
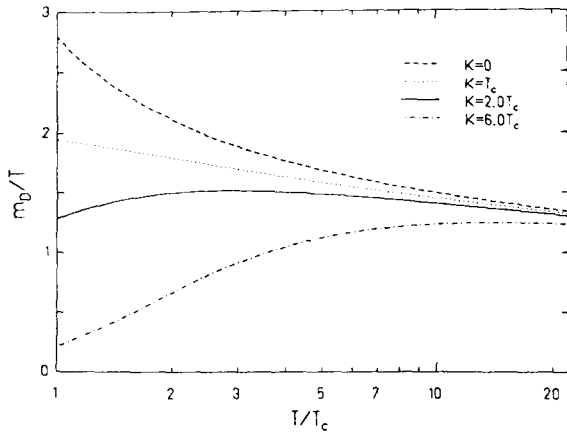
Fig. 1. The Debye screening mass as a function of temperature $T$ for $K=0$ (dashed line), $K=T_c$ (dotted line), $K=2T_c$ (solid line) and $K=6T_c$ (dash-dotted line).
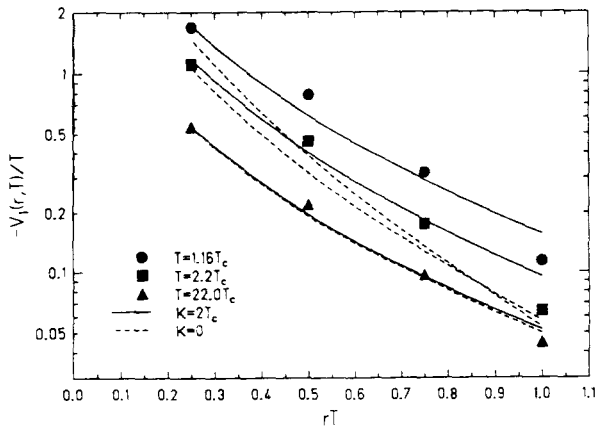


Fig. 2. The function $-V_1(r, T)/T$ versus lattice distance $rT$ at $T=2.2T_c$ (squares), $T=22.0T_c$ (triangles) and $T=1.16T_c$ (circles). The points are MC data [10], the solid lines correspond to the cut-off model at $K=2T_c$, while the dashed ones represent the standard perturbative calculations with $K=0$.

smaller at $T$ near $T_c$ because of the low-momentum cut-off, and according to eqs. (2), (3) the range of all potentials grows. This is just what is needed to describe the singlet potential. In fig. 2 the MC data for $-V_1/T$ are compared with eq. (2): the standard perturbative results ($K=0$) and the cut-off model at $K=2T_c$. One can see the strong deviation (at small $T$ and large $r$) of MC data from the $K=0$ fit and a much better description of the $r$-dependence with $K=2T_c$. The absolute normalization of $V_1$ given in terms of

$g^2(T; K)$ (4) without any additional free parameter is also in good agreement with MC data.

Calculating $V_1$ and $V_8$ in the cut-off model (2)–(7) and then $V$ from eq. (1) we find a disagreement of the MC data with the colour-averaged potential $V$ both for $K=0$ and $K=2T_c$. MC data for $V$ suggest a very large value of the cut-off parameter: $K=6T_c$ (see fig. 3). It just means that relations (8), (9) are violated. Indeed, MC data [10] show the strong violation of (9) even at very high temperature, $T=22.0T_c$. The reason for this can be seen from the expansion of the exponential functions in eq. (1). The relation (9) follows from eqs. (2), (3) due to the cancellation of the linear $-V_1/T$ and $8V_8/T$ terms in $-V/T$. These terms are of order $g^2$ and their absolute values are much larger than the order $g^4$ contribution, which determines $-V/T$. Therefore, even a small violation of the relation (8) can lead to a large discrepancy in relation (9).

We face a somewhat unexpected situation: the singlet potential can be rather well described in the cut-off model with $K=2T_c$, but this gives no agreement of the model with MC data for the colour-averaged potential (relation (8) and especially (9) are strongly violated). A possible explanation of these facts is that there are substantially *different* non-perturbative contributions to the singlet and octet potentials. Indeed, we find that MC data for $V_8$ cannot be fitted
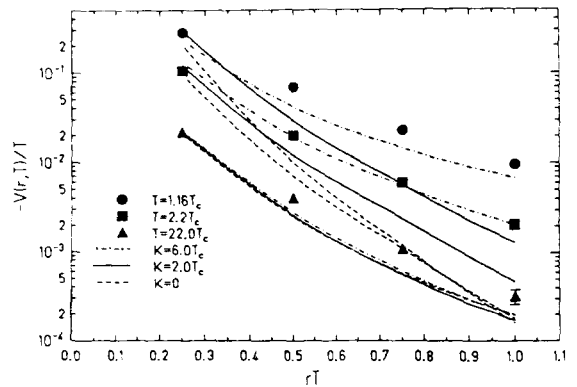


Fig. 3. The function $-V(r, T)/T$ versus lattice distance $rT$ at $T=1.16T_c$ (circles), $T=2.2T_c$ (squares) and $T=22.0T_c$ (triangles). The points are MC data [10], the solid and dash-dotted lines correspond to eq. (1) with the cut-off model for singlet potential (2) and octet potential (3) at $K=2T_c$ and $K=6T_c$, while the dashed ones represent the standard perturbative calculations with $K=0$ for $V_1$ and $V_8$.

with $K=2T_c$, but $K=0$ leads to a good description (see fig. 4). It is seen from figs. 2 and 4 that even the best fit curves do not quite correctly describe the "curvature" of the potentials. One can try to improve this behaviour introducing an additional $r$-dependence of the coupling constant, but we do not discuss this possibility.

With the "mixed" description ($K=2T_c$ for $V_1$ in eq. (2) and $K=0$ for $V_8$ in eq. (3)) we obtain using eq. (1) a rather good agreement with the colour-averaged potential $V$ (see fig. 5). More than that, MC data for $-V_1/V_8$ and $-V_1^2/TV$ ratios are fitted now with a reasonable accuracy (see figs. 6, 7)! We stress that the assumption of different values of $K$ for $V_1$ and $V_8$ is the only possibility to fit MC data for $-V_1/V_8$ and $-V_1^2/TV$. These ratios are also important because we expect a (partial) cancellation of the finite size effects in MC data for them.

We summarise our analysis as follows. The standard perturbative calculations ($K=0$) cannot reproduce the singlet potential $V_1$ (fig. 2), the colour-averaged potential $V$ (fig. 3) and the $-V_1/V_8$, $-V_1^2/TV$ ratios (figs. 6, 7). The cut-off model with $K=2T_c$ fits MC data for the singlet potential $V_1$ (fig. 2) but fails to describe the other ones. With $K=6T_c$ (meaning very strong non-perturbative effects) one can describe MC data for the colour-averaged potential (see fig. 3), but this value of $K$ leads to a disagreement with MC data both for $V_1$ and $V_8$ (see figs. 2 and 4).
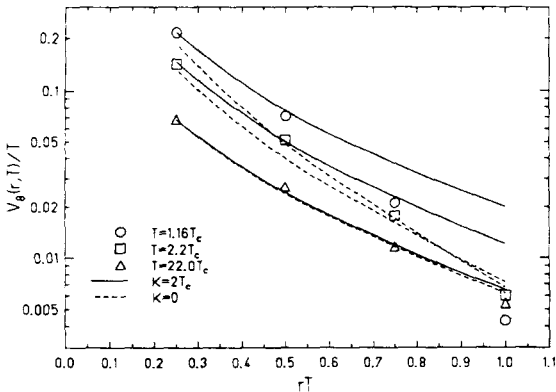


Fig. 4. The function $V_8(r, T)/T$ versus lattice distance $rT$ at (a) $T=2.2T_c$ (open squares) and $T=22.0T_c$ (open triangles), (b) $T=1.16T_c$ (open circles). The points are MC data [10], the solid lines correspond to the cut-off model at $K=2T_c$, while the dashed ones represent the standard perturbative calculations with $K=0$.
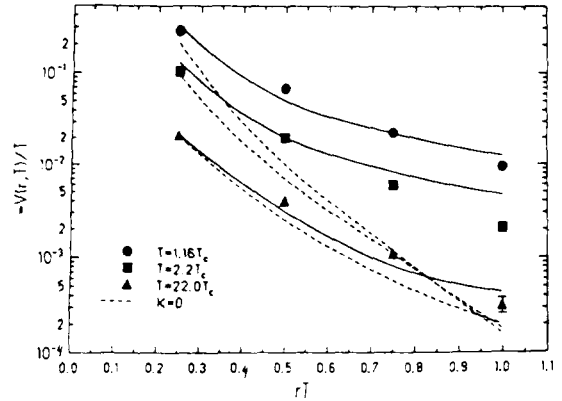


Fig. 5. The same as in fig. 3, but the solid lines correspond to eq. (1) with the cut-off model for singlet potential (2) at $K=2T_c$ and octet potential (3) at $K=0$. The dashed ones represent the standard perturbative calculations with $K=0$ for $V_1$ and $V_8$.
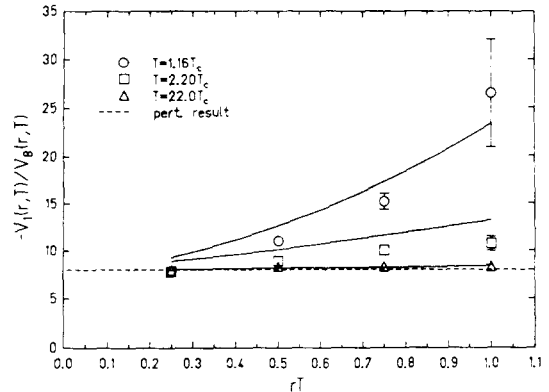


Fig. 6. The ratio $-V_1(r, T)/V_8(r, T)$ versus $rT$. The points are MC data [10] for $T=22.0T_c$, $T=2.20T_c$ and $T=1.16T_c$. The solid lines correspond to the cut-off model for singlet potential (2) at $K=2T_c$ and octet potential (3) at $K=0$. The dashed ones represent the standard perturbative result.

Besides, with any value of $K$ one would expect the standard perturbative relations (8), (9) to be valid. MC data, however, strongly violate them (figs. 6, 7). Therefore, only the "mixed" description with $K=2T_c$ for $V_1$ and $K=0$ for $V_8$ leads to a good fit of all potentials.

In previous studies attention was mainly paid to the colour-averaged potential and it was concluded that MC data show very strong non-perturbative effects. Non-perturbative effects are probably large even at high temperatures if the length scale $r \gg 1/T$ is important. However, our analysis deals with $rT \leqslant 1$, and
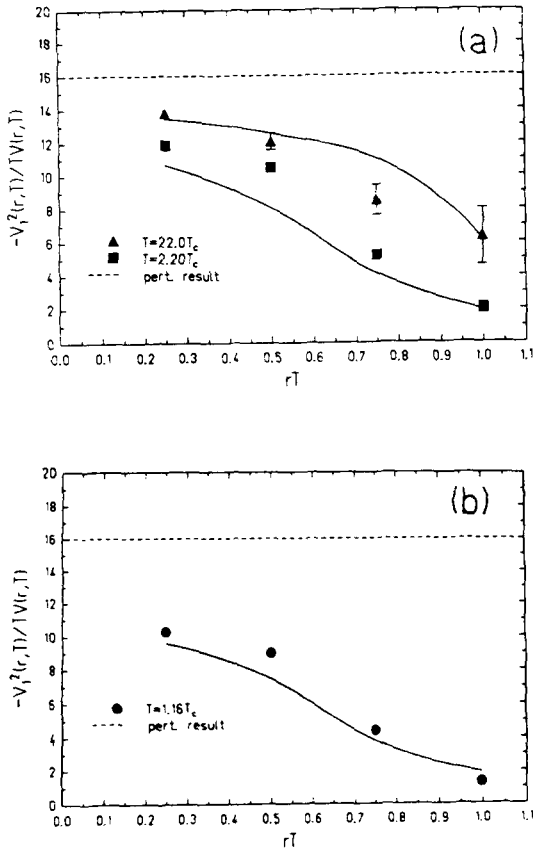
Fig. 7. The ratio $-V_1^2(r, T)/TV(r, T)$ versus $rT$. The points are MC data [10] for (a) $T=22.0T_c$, $T=2.20T_c$, and (b) $T=1.16T_c$. The solid lines correspond to eq. (1) for $V(r, T)$ in the cut-off model for singlet potential (2) at $K=2T_c$ and octet potential (3) at $K=0$. The dashed ones represent the standard perturbative result.

standard perturbative formula, where the low-momentum gluons contribute. However, the octet state carries an open colour and consequently, the "quasi-confining" interaction tries to neutralize it with the low-momentum gluons. Therefore, such gluons are not forbidden in the vicinity of the QQ̄ octet state.

we expect rather moderate non-perturbative corrections. Indeed, we have shown that the failure of the previous attempts to describe perturbatively the colour-averaged potential and $-V_1/V_8$, $-V_1^2/TV$ ratios happened not because the non-perturbative corrections to $V_1$ and $V_8$ are very large (in fact, we have not found the presence of the non-perturbative corrections to the octet potential) but because they are different in the singlet and octet colour channels.

Finally, let us speculate on the physical interpretation of these results. The "quasi-confining" interaction in the GP transforms low-momentum gluons into massive colourless states [18]. The behaviour of the singlet potential seems to support this picture. On the other hand the octet potential is well described by the

## References

[1] T.A. DeGrand and C.E. DeTar, Phys. Rev. D 34 (1986) 2469.
[2] F. Karsch, Z. Phys. C 38 (1988) 147.
[3] J. Engels, J. Fingberg, F. Karsch, D. Miller and M. Weber, Phys. Lett. B 252 (1990) 625.
[4] M.I. Gorenstein and O.A. Mogilevsky, Z. Phys. C 38 (1988) 161.
[5] J. Engels, J. Fingberg, K. Redlich, H. Satz and M. Weber, Z. Phys. C 42 (1989) 341.
[6] M.I. Gorenstein and O.A. Mogilevsky, Phys. Lett. B 228 (1989) 121.
[7] D.H. Rischke, J. Schaffner, M.I. Gorenstein, A. Schäfer, H. Stöcker and W. Greiner, Frankfurt preprint UFTP-284 (1991).
[8] M.I. Gorenstein, O.A. Mogilevsky and S. Mrówczyński, Phys. Lett. B 246 (1990) 200.
[9] J. Engels, F. Karsch and H. Satz, Nucl. Phys. B 315 (1989) 419.
[10] N. Attig, F. Karsch, B. Petersson, H. Satz and M. Wolff, Phys. Lett. B 209 (1988) 65.
[11] L.D. McLerran and B. Svetitsky, Phys. Rev. D 24 (1981) 450;
S. Nadkarni, Phys. Rev. D 33 (1986) 3738; D 34 (1986) 3904.
[12] J. Hoek, Nucl. Phys. B 339 (1990) 732.
[13] J.I. Kapusta, Nucl. Phys. B 148 (1979) 461.
[14] H.-Th. Elze and U. Heinz, Phys. Rep. 183 (1989) 81.
[15] S. Mrówczyński, Phys. Rev. D 39 (1989) 1940; in: Direction in high energy physics, quark–gluon plasma, ed. R. Hwa (World Scientific, Singapore).
[16] A. Hasenfratz and P. Hasenfratz, Phys. Lett. B 93 (1980) 165.
[17] T. Hatsuda, Invited talk Intern. Symp. on High energy nuclear collisions and quark–gluon plasma (Kyoto, Japan, June 1991).
[18] C. DeTar, Phys. Rev. D 32 (1985) 276;
E. Manousakis and J. Poloni, Phys. Rev. Lett. 58 (1987) 847;
J.B. Kogut and C. DeTar, Phys. Rev. D 36 (1987) 847.